Online ISSN 1848-3380, Print ISSN 0005-1144
ATKAFF 56(1), 21–32(2015)

Sandeep Gupta, Ramesh Kumar Tripathi

Transient Stability Assessment of Two-Area Power System with LQR based CSC-STATCOM

DOI 10.7305/automatika.2015.04.644
UDK 621.311.16.016.35.051.025.076.1:681.516.3

Original scientific paper

A current source converter (CSC) based static synchronous compensator (STATCOM) is a shunt flexible AC transmission system (FACTS) device, which has a vital role as a stability support for small and large transient instability in an interconnected power network. A robust linear quadratic regulator (LQR) based controller for CSC-STATCOM is proposed. In this paper, LQR based CSC-STATCOM is designed to enhance the transient stability of two-area two-machine power system. First of all, modeling & LQR based controller design for CSC-STATCOM are described. After that, the impact of the proposed scheme on the test system with different disturbances is demonstrated. The feasibility of the proposed scheme is demonstrated through simulation in MATLAB and the simulation results show an improvement in the transient stability of power system with CSC-STATCOM. Also, the robustness and effectiveness of CSC-STATCOM are better rather than other shunt FACTS devices (SVC & VSC-STATCOM) in this paper.

Key words: CSC, EAC (equal area criterion), FACTS, LQR, STATCOM

Procjena prijelazne stabilnosti dvopodručnog energetskog sustava s CSC-STATCOM-om zasnovanom na LQR-u. Statički sinkroni kompenzator (STATCOM) zasnovan na pretvaraču strujnog izvora (CSC) je uređaj za izmjenični prijenos s fleksibilnim "shuntom" (FACTS), koji značajno doprinosi stabilnosti malih i srednjih prijelaznih nestabilnosti u međusobno povezanoj energetskoj mreži. Ovdje je predložen robusni sustav upravljanja zasnovan na linearnom kvadratičnom regulatoru (LQR) za CSC-STATCOM. U ovom radu, CSC-STATCOM zasnovan na LQR-u dizajniran je za povećanje stabilnosti dvopodručnog energetskog sustava s dva motora. Prvo su opisani postupak modeliranja te upravljački sustav zasnovan na LQR-u za CSC-STATCOM. Nakon toga, prikazan je utjecaj predstavljene sheme na ispitni sustav uz prisutnost različitih poremećaja. Provedivost predstavljenog pristupa je prikazana kroz MATLAB simulacije čiji rezultati prikazuju poboljšanje u prijelaznoj stabilnosti energetskog sustava s CSC-STATCOM-om. Također, u ovom radu je prikazana veća robusnost i efikasnost CSC-STATCOM "shunt" FACTS uređaja u odnosu na SVC & VSC-STATCOM.

Ključne riječi: CSC, EAC (kriterij jednakih površina), FACTS, LQR, STATCOM

1 INTRODUCTION

The continuous enhancement of electrical loads due to the modernization of the society results in transmission structure to be operated near to their stability restrictions. So the renovation of urban and rural power network becomes necessary. Due to governmental, financial and green climate reasons, it is not always possible to construct new transmission lines to relieve the power system stability problem at the existing overloaded transmission lines. As a result, the utility industry is facing the challenge of efficient utilization of the existing AC transmission lines in power system networks. So transient stability, voltage regulation, damping oscillations etc. are the most important operating issues that electrical engineers are facing during power-transfer at high levels.

In above power quality problems, transient stability is the one of the most important key factor during power-transfer at high levels. According to the literature, transient stability of a power system is its ability to maintain synchronous operation of the machines when subjected to a large disturbance [1]. While the generator excitation system can maintain excitation control but it is not adequate to sustain the stability of power system due to faults or overloading near to the generator terminals [2].

Therefore researchers are working on this problem long time to find the solution. These solutions are such as using wide-area measurement signals [3], phasor measurement unit [4] and flexible AC transmission system etc. In these solutions, one of the powerful methods for enhancing the transient stability is to use flexible AC transmission sys-

tem (FACTS) devices [5-8]. Even though the prime objective of shunt FACTS devices (SVC, STATCOM) is to maintain bus voltage by absorbing (or injecting) reactive power, they are also competent of improving the system transient stability by diminishing (or increasing) the capability of power transfer when the machine angle decreases (increases), which is accomplished by operating the shunt FACTS devices in inductive (capacitive) mode.

In many cited research papers [2, 9-11], the different types of these devices and with different control techniques are used for improving transient stability. Among these devices, the STATCOM is valuable for enhancement stability and frequency stabilization due to the rapid output response, lower harmonics, superior control stability and small size etc. [8, 12, 13]. By their inverter configuration, basic Type of STATCOM topology can be realized by either a current-source converter (CSC) or a voltage-source converter (VSC) [13-17]. But recent research confirms several merits of CSC based STATCOM over VSC based STATCOM [18-20]. These advantages are high converter reliability, quick starting, inherent short-circuit protection, the output current of the converter is directly controlled and in low switching frequency this reduces the filtering requirements compared with the case of a VSC. Therefore CSC based STATCOM is very useful in power system rather than VSC based STATCOM in many cases.

Presently the most used techniques for controller design of FACTS devices are the Proportional Integration (PI), PID controller [21], pole placement and linear quadratic regulator (LQR) [22]. But LQR and pole placement algorithms give quicker response in comparison to PI & PID algorithm and LQR is the optimal theory of pole placement method and describes the optimal pole location based on two cost function [23]. So LQR method has better performance among these methods.

The main contribution of this paper is the application of LQR based CSC-STATCOM for transient stability improvement of power system by injecting (or absorbing) reactive power. In this paper, the proposed LQR controller based CSC-STATCOM is used in Two area power system with dynamic load under serious disturbance conditions (three phase fault or heavy loading) to enhancement of transient stability studies and observe impact of the CSC-STATCOM on electromechanical oscillations and transmission capacity. More ones, the resulting outcomes from the proposed algorithm based CSC-STATCOM are compared to that obtained from the other shunt FACTS devices (SVC & VSC based STATCOM) which are used in previous works [24, 25].

The rest of paper is prepared as follows. Section-2 discusses about the circuit modeling & LQR controller designing of CSC based STATCOM. A two-area two-machine power system is described with a CSC-STATCOM device in Section-3. Simulation results of the test system with & without CSC based STATCOM for severe contingency are shown in Section-4, to improve the transient stability of the system. Comparison among the performance of different shunt FACTS devices such as SVC, VSC-STATCOM and CSC-STATCOM is also presented in Section-4. Finally, Section-5 concludes this paper.

2 MATHEMATICAL MODELING OF LQR BASED CSC-STATCOM

2.1 CSC based STATCOM model

To verify the response of the CSC-STATCOM on dynamic performance, the mathematical modeling and control strategy of a CSC based STATCOM are presented. So in the design of controller for CSC based STATCOM, the state space equations from the CSC based STATCOM circuit is introduced. To minimize the complexity of mathematical calculation, the theory of dq transformation of currents has been applied in this circuit, which makes the d and q components as independent parameters. Fig. 1 shows the circuit diagram of a typical CSC based STATCOM.

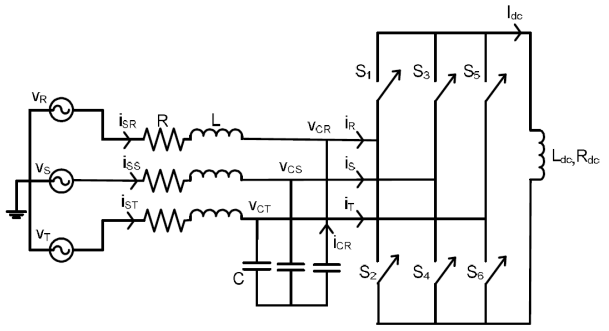

Fig. 1. The representation of CSC based STATCOM

Where

i_{SR}, i_{SS}, i_{ST} line current;

v_{CR}, v_{CS}, v_{CT} voltages across the filter capacitors;

v_R, v_S, v_T line voltages;

I_{dc} dc-side current;

R_{dc} internal resistance of the dc-link inductor (converter switching and conduction losses);

L_{dc} smoothing inductor (dc-link);

C filter capacitance;

L inductance of the line reactor;

R resistance of the line reactor

The basic mathematical equations of the CSC based STATCOM have been derived from the literature [20]. Therefore, only brief details of the primary equations for CSC-STATCOM are given here for the readers' convenience. Based on the equivalent circuit of CSC-STATCOM as shown in Fig.1, the differential equations for the system can be achieved, which are derived in the abc frame and then transformed into the synchronous dq frame using dq transformation method [26].

$$\frac{d}{dt}I_{dc} = -\frac{R_{dc}}{L_{dc}}I_{dc} - \frac{3}{2L_{dc}}M_dV_d - \frac{3}{2L_{dc}}M_qV_q \quad (1)$$

$$\frac{d}{dt}I_d = -\frac{R}{L}I_d + \omega I_q - \frac{1}{L}\frac{E_d}{n} + \frac{1}{L}V_d \quad (2)$$

$$\frac{d}{dt}I_q = -\omega I_d - \frac{R}{L}I_q + \frac{1}{L}V_q \quad (3)$$

$$\frac{d}{dt}V_d = -\frac{1}{C}I_d + \omega V_q + \frac{1}{C}M_dI_{dc} \quad (4)$$

$$\frac{d}{dt}V_q = -\frac{1}{C}I_q - \omega V_d + \frac{1}{C}M_qI_{dc} \quad (5)$$

In above differential equations M_d and M_q are the two input variables. Two output variables are I_{dc} and I_q. Here, ω is the rotation frequency of the system and this is equal to the nominal frequency of the system voltage. I_d & I_q are the d-axis & q-axis components of the line current. M_d & M_q are d-axis & q-axis components of the system modulating signal (m), respectively. Here $M_d = m \cdot \cos\theta$ and $M_q = m \cdot \sin\theta$ (where θ is the phase angle of converter output current). E_d & E_q are direct & quadrature axis of the system voltage. Here E_d is taken as the RMS value of the system voltage and E_q is taken as a zero. V_d & V_q are the d-axis & q-axis components of the voltage across filter capacitor, respectively.

Equation (1) is shown that controller for CSC based STATCOM has nonlinearity characteristic. So this nonlinear property can be removed by accurately modeling of CSC based STATCOM. From equations (1)-(5), it can be seen that nonlinear property in the CSC-STATCOM model is due to the part of I_{dc}. This nonlinear property is removed with the help of active power balance equation. Here, it has been assumed that the power loss in the switches and resistance R_{dc} is ignored and the turns ratio of the shunt transformer is $n : 1$. After using power balance equation and mathematical calculation, nonlinear characteristic is removed from the equation (1). Finally the equation is obtained below:

$$\frac{d}{dt}\left(I_{dc}^2\right) = -\frac{2R_{dc}}{L_{dc}}\left(I_{dc}^2\right) - \frac{3E_d}{L_{dc}n}I_d \quad (6)$$

In the equation (6) state variable (I_{dc}) is replaced by the state variable (I_{dc}^2), to make the dynamic equation linear. Finally the resulting better dynamic and robust model of the CSC-SATACOM in matrix form can be derived as:

$$\frac{d}{dt}\begin{bmatrix} (i_{dc})^2 \\ i_d \\ i_q \\ v_{cd} \\ v_{cq} \end{bmatrix} = \begin{bmatrix} -\frac{2R_{dc}}{L_{dc}} & \frac{3E_d}{L_{dc}n} & 0 & 0 & 0 \\ 0 & -\frac{R}{L} & \omega_o & \frac{1}{L} & 0 \\ 0 & -\omega_o & -\frac{R}{L} & 0 & \frac{1}{L} \\ 0 & -\frac{1}{C} & 0 & 0 & \omega_o \\ 0 & 0 & -\frac{1}{C} & -\omega_o & 0 \end{bmatrix} * \begin{bmatrix} (i_{dc})^2 \\ i_d \\ i_q \\ v_{cd} \\ v_{cq} \end{bmatrix} + \begin{bmatrix} 0 & 0 \\ 0 & 0 \\ 0 & 0 \\ \frac{1}{C} & 0 \\ 0 & \frac{1}{C} \end{bmatrix} * \begin{bmatrix} I_{id} \\ I_{iq} \end{bmatrix} + \begin{bmatrix} 0 \\ -\frac{1}{L} \\ 0 \\ 0 \\ 0 \end{bmatrix} * E_d \quad (7)$$

Above modeling of CSC based STATCOM is written in the form of modern control methods i.e. State-space representation. For state-space modeling of the system, section 2.2 has been considered.

2.2 LQR controller Design

Linear Quadratic Regulator (LQR) theory is no doubt one of the most basic control system design methods. LQR algorithm is the optimal theory of pole placement method and picks the best possible pole location based on the two cost functions. This method finds the optimal feedback gain matrix that reduces the cost function. One way of representing the quadratic cost function in mathematics for LQR formulation is below:

$$J = \int_0^\infty x^T Q x dt + \int_0^\infty u^T R u dt \quad (8)$$

Here Q and R are the symmetric, non-negative definite weighting matrices.

In the dynamic modeling of system, State-space equations involve three types of variables: state variables (x), input (u) and output (y) variables with disturbance (e). So comparing (7) with the standard state-space representation i.e.

$$\dot{x} = Ax + Bu + Fe \quad (9)$$

$$y = Cx \quad (10)$$

where the system matrices as:

$$x = \begin{bmatrix} I_{dc}^2 & I_d & I_q & V_d & V_q \end{bmatrix}^T; u = \begin{bmatrix} I_{id} & I_{iq} \end{bmatrix}^T$$

$$e = E_d; y = \begin{bmatrix} I_{dc}^2 & I_q \end{bmatrix}^T$$

$$A = \begin{bmatrix} -\frac{2R_{dc}}{L_{dc}} & -\frac{3E_d}{L_{dc}} & 0 & 0 & 0 \\ 0 & -\frac{R}{L} & \omega & \frac{1}{L} & 0 \\ 0 & -\omega & -\frac{R}{L} & 0 & \frac{1}{L} \\ 0 & -\frac{1}{c} & 0 & 0 & \omega \\ 0 & 0 & -\frac{1}{c} & -\omega & 0 \end{bmatrix}$$

$$B = \begin{bmatrix} 0 & 0 \\ 0 & 0 \\ 0 & 0 \\ \frac{1}{c} & 0 \\ 0 & \frac{1}{c} \end{bmatrix}; C = \begin{bmatrix} 1 & 0 \\ 0 & 0 \\ 0 & 1 \\ 0 & 0 \\ 0 & 0 \end{bmatrix}^T; F = \begin{bmatrix} 0 \\ -\frac{1}{L} \\ 0 \\ 0 \\ 0 \end{bmatrix}$$

Equations (9) & (10) represent five system states, two control inputs and two control outputs. Where, x is the state vector, u is the input vector, A is the basis matrix, B is the input matrix, e is disturbance input.

Now in the presence of disturbance the control equation can be formulated as:

$$u = -K * x + J * y_{ref} + N * e \tag{11}$$

Then the state equation of closed loop is modified as

$$\dot{x} = (A - B * K) * x + J * y_{ref} + B * N * e + F * e \tag{12}$$

Where K is the state-feedback matrix, N is the feedback matrix for the disturbance input, y_{ref} is the reference input, and J is a diagonal matrix which is used to obtain the unity steady-state gain. The matrix N should be designed in such a way that the output y should be minimally influenced by the disturbance e. This objective can be achieved by making:

$$\lim_{s \to 0} C(s * I - A + B * K)^{-1}(B * N + F) = 0 \ \& \ \dot{x} = 0$$

Therefore J & N values are found out from a mathematical calculation for tracking the reference output value (y_{ref}) by the system output value (y). For computation of these values, two equations are used such as:

$$J = [C * (-(A - B * K)^{-1}) * B]^{-1}$$

and

$$N = [C * (-A + B * K)^{-1} * B]^{-1} * \\ *[C * (-A + B * K)^{-1} * F]$$

.

Here y_{ref} can be written as below:

$$y_{ref} = \begin{bmatrix} I^2_{dc(ref)} \\ I_{q(ref)} \end{bmatrix}$$

In order to, reduce the cost function (performance index) and to achieve the best value of gain matrices K, following two equations are used.

$$K = R^{-1} B^T P \tag{13}$$

$$A^T P + PA - PBR^{-1} B^T P + Q = 0 \tag{14}$$

Equation (14) is also called the algebraic riccati equation [27]. The final configuration of the proposed LQR based CSC-STATCOM is shown in Fig. 2.

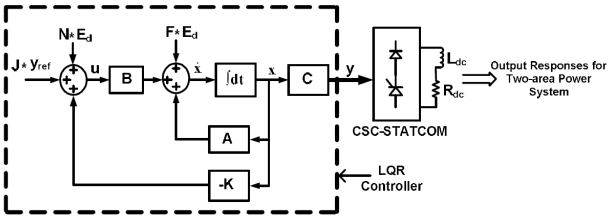

Fig. 2. Control Structure of LQR based CSC-STATCOM

3 TWO-AREA POWER SYSTEM WITH CSC-STATCOM FACTS DEVICE

In order to observe the performance of proposed LQR controller in the previous section, a two-area two-machine power system with a CSC-STATCOM is considered, The CSC-STATCOM is connected at bus b through a long transmission system as shown in Fig. 3. Figure 3(b) represents the equivalent circuit of test system without CSC-STATCOM. The active power flows from area 1 to area 2. Figure 3(c) represents the equivalent circuit of the test system with a CSC-STATCOM, where CSC-STATCOM is used as shunt current source device.

The dynamic model of the machine, with a CSC-STATCOM, can be written in the differential algebraic equation form as follows:

$$\dot{\delta} = \omega \tag{15}$$

$$\dot{\omega} = \frac{1}{M} \left[P_m - P_{eo} - P_e^{\text{csc}} \right] \tag{16}$$

Here ω is the rotor speed, δ is the rotor angle, P_m is the mechanical input power of generator, the output electrical power without CSC-STATCOM is represents by P_{eo} and M is the moment of inertia of the rotor. Equation (16) is also called as swing equation. The additional factor of the output electrical power of generator from a CSC-STATCOM is P_e^{csc} in the swing equation. From Fig. 3(b), output of generator (P_{eo}) is

$$P_{eo} = \frac{E_1 V_{bo}}{X_1} \sin(\delta - \theta_{bo}) = \frac{E_1 E_2}{X_1 + X_2} \sin(\delta) \tag{17}$$

Where V_{bo} and θ_{bo} are voltage magnitude and angle at bus b in the absence of CSC-STATCOM, which are computed as follows:

$$\theta_{bo} = \tan^{-1} \left[\frac{X_2 E_1 \sin \delta}{X_2 E_1 \cos \delta + X_1 E_2} \right] \tag{18}$$

$$V_{bo} = \left(\frac{X_2 E_1 \cos(\delta - \theta_{bo}) + X_1 E_2 \cos\theta_{bo}}{X_1 + X_2} \right) \quad (19)$$

For calculation of P_e^{csc}, Fig. 3(c) is considered and assumed that CSC-STATCOM is working in capacitive mode. The injected current from CSC-STATCOM to test system can be written as:

$$I_{\text{csc}} = I_{\text{csc}} \angle(\theta_{bo} - 90^o) \quad (20)$$

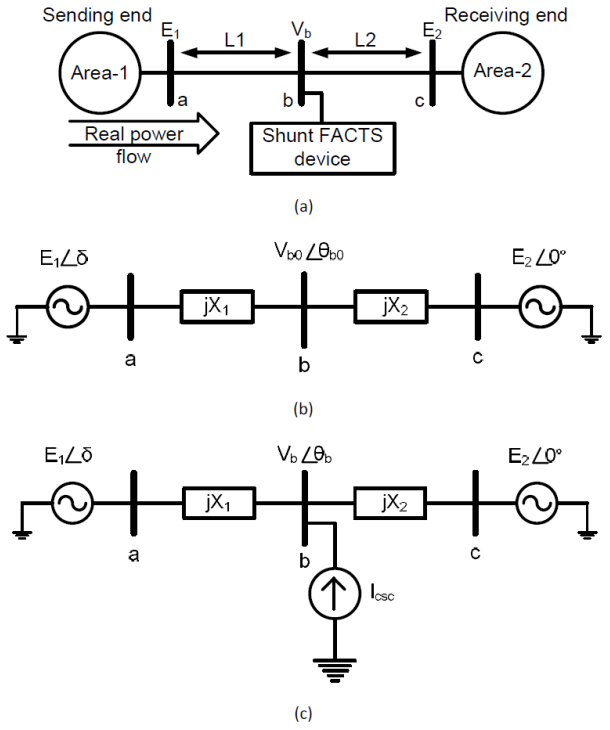

Fig. 3. A two-area two-machine power system with CSC-STATCOM; (a) A single line diagram; (b) Simplified model of the test system without CSC-STATCOM; (c) Simplified model of the test system with a CSC-STATCOM as a current injection device

In Fig. 3(c), the magnitude (V_b) and angle (θ_b) of voltage at bus b can be computed as:

$$\theta_b = \tan^{-1}\left[\frac{X_2 E_1 \sin\delta}{X_2 E_1 \cos\delta + X_1 E_2} \right] \quad (21)$$

$$V_b = \left(\frac{X_2 E_1 \cos(\delta - \theta_{bo}) + X_1 E_2 \cos\theta_{bo}}{X_1 + X_2} \right) + \left(\frac{X_1 X_2}{X_1 + X_2} I_{\text{csc}} \right) \quad (22)$$

From equation (22), it can be said that the voltage magnitude of bus b (V_b) depends on the STATCOM current (I_{csc}). In Fig. 3(c), the electrical output power P_e^{csc} of machine due to a CSC-STATCOM, can be expressed as:

$$P_e^{\text{csc}} = \frac{E_1 V_b}{X_1} \sin(\delta - \theta_b) \quad (23)$$

Finally, using equations (22) & (23) the total electrical output (P_e) of machine with CSC-STATCOM can be written as

$$P_e = P_{eo} + P_e^{\text{csc}} \Rightarrow$$
$$P_e = P_{eo} + \frac{X_1 X_2 E_1}{(X_1 + X_2) X_1} I_{\text{csc}} \sin(\delta - \theta_b) \quad (24)$$

All above equations are represented for the capacitive mode of CSC-STATCOM. For the inductive mode of operation negative value of I_{csc} can be substituted in equations (20), (22) & (24) in place of positive I_{csc} . With the help of equation (16), the power-angle curve of the test system can be drawn for stability analysis as shown in Fig. 4.

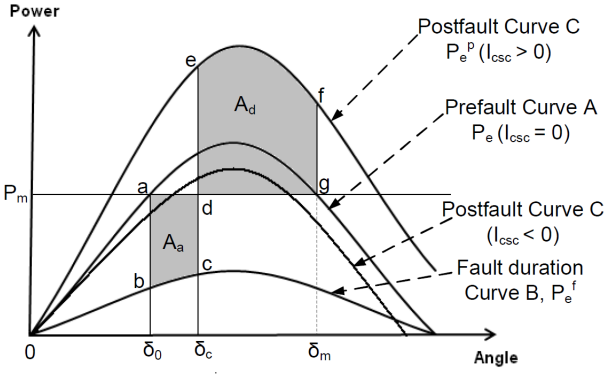

Fig. 4. Power-Angle characteristic of the test system with a CSC-STATCOM

The power-angle ($P - \delta$) curve of the test system without a CSC-STATCOM is represented by curve A (also called prefault condition) in Fig. 4. Here the mechanical input is P_m , electrical output is P_e and initial angle is δ_0. When a fault occurs, P_e suddenly decreases and the operation shifts from point a to point b at curve B and thus the machine starts accelerating from point b to point c, where accelerating power (P_a) is positive. Here accelerating power (P_a) is the difference between mechanical input (P_m) & electrical output (P_e) power. At fault clearing, P_e suddenly increased and the area a-b-c-d-a represents the accelerating area A_a as defined in equation (25). If the CSC-STATCOM operates in a capacitive mode (at fault clearing), P_e increases to point e at curve C (also called postfault condition). At this time P_a is negative. Thus the machine starts decelerating but its angle continues to increase from point e to the point f until reaches a maximum

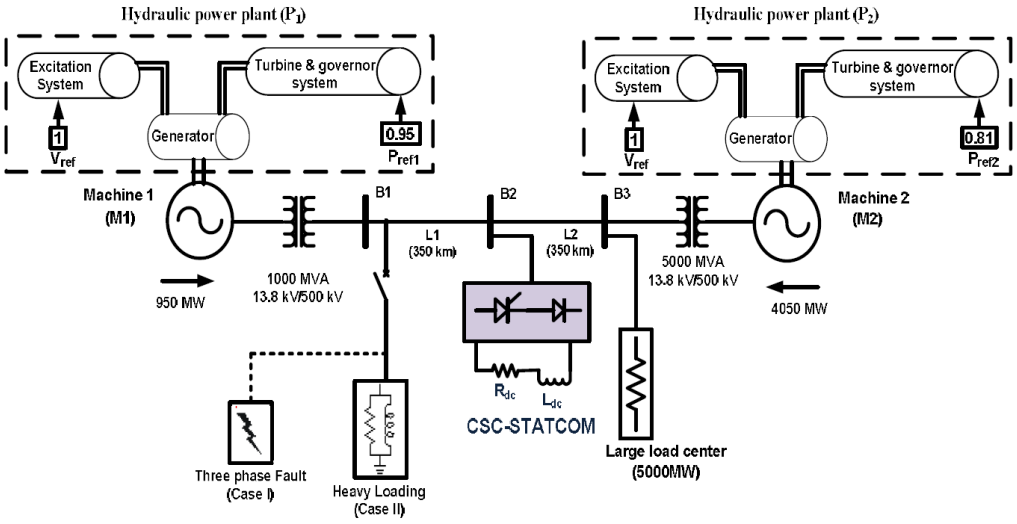

Fig. 5. The single line diagram of the test-system model for transient stability study of two power plants (P1 & P2)

allowable value δ_m at point f, for system stability. The area e-f-g-d-e represents the decelerating area A_d as defined in equation (25). From previous literature [1], equal area criterion for stability of the system can be written as:

$$\int_{\delta_0}^{\delta_c} \left(P_m - P_e^f\right) d\delta = \int_{\delta_c}^{\delta_m} \left(P_e^p - P_m\right) d\delta \Rightarrow A_a = A_d \tag{25}$$

This equation is generated from Fig. 4, where δ_c is critical clearing angle. P_e^p is an electrical output for post-fault condition. P_e^f is an electrical output during fault condition. From Fig. 4, it is seen that for capacitive mode of operation ($I_{\text{csc}} > 0$), the $P - \delta$ curve is not only lifted up but also displaced toward right and that endues more decelerating area and hence higher stability limit. Now in the following section transient stability of two-area two-machine power system is analyzed using the proposed LQR based controller with CSC-STATCOM.

4 SIMULATION RESULTS

4.1 Power system under study:

In this section, two-area power system is considered as test system for study. For this type of test system, a 500-kV transmission system with two hydraulic power plants P_1 (machine-1) & P_2 (machine-2) connected through 700-km long transmission line is taken as shown in Fig. 5. Rating of first power generation plant (P_1) is $13.8\,\text{kv}/1000\,\text{MVA}$, which is used as P_V generator bus type. The electrical output of the second power plant (P_2) is $5000\,\text{MVA}$, which is used as a swing bus for balancing the power. One $5000\,\text{MW}$ large resistive load is connected near the plant P_2 as shown in Fig. 5. To maintain the synchronism of plants (i.e. machines 1 & 2) and improved the transient stability of the test system after disturbances (faults or heavy loading), a LQR based CSC-STATCOM is connected at the mid-point of transmission line (at bus B2). Achieve maximum efficiency; CSC-STATCOM is connected at the mid-point of transmission line, as per [28]. The two hydraulic generating units are assembled with a turbine-governor set and excitation system, as explained in [1]. Power oscillation damping (POD) unit is not used with shunt FACTS device. All the data required for this test system model are mentioned in Appendix A.

The impact of the LQR controller based CSC-STATCOM has been observed for maintaining the system stability through MATLAB/SIMULINK. Severe contingencies such as short-circuit fault and instant loading, are considered.

4.2 Case I-Short-Circuit Fault:

A three-phase fault is created at near bus B1 at $t = 0.1\,\text{s}$ and is cleared at $0.23\,\text{s}$. The impact of system with & without CSC based STATCOM, due to this disturbance are shown in Figs. 6 to 11. Simulations are carried out for 8 s to observe the nature of transients. From Figs. 6 & 7, it is observed that the system without CSC-STATCOM is unstable even after the clearance of the fault. But the same system with LQR based CSC-STATCOM is restored and stable after the clearance of the fault as observed from Figs. 8 to 11.

Synchronism between two machines M1 & M2 is also maintained as shown in Figs. 9 & 10. CCT is defined as the maximal fault duration for which the system remains transiently stable [1]. The critical clearing time (CCT) of fault

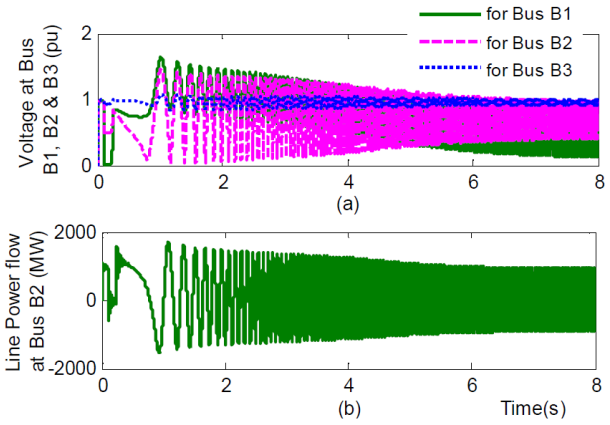

Fig. 6. Test system response without CSC-STATCOM for a three phase fault (Case-I). (a) Positive sequence voltages at different buses B1, B2 & B3 (b) Power flow at bus B2

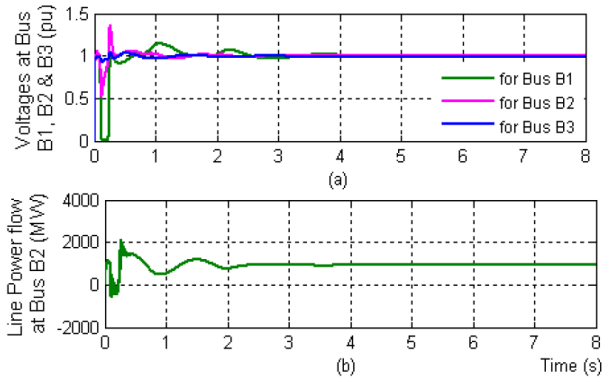

Fig. 7. System response without CSC-STATCOM for Case-I (a) Difference between Rotor angles of machines M1 & M2 (b) w1 & w2 speeds of machine M1 & M2 respectively (c)terminal voltages Vt1 & Vt2 of generators M1 & M2 respectively

is also found out for the test system stability by simulation. The fault time is increased to find the critical stability margin, thus CCT is obtained. CCT of the fault for system with & without CSC-STATCOM are 286 ms and 222 ms respectively, as shown in Table-1. It is observed that CCT of fault is also increased due to the impact of LQR based CSC-STATCOM.

4.3 Case II-Large Loading:

For heavy loading case, a large load (10000 MW/5000 Mvar) is connected at near bus B1 (i.e. at near plant P_1) in Fig. 5. This loading occurs during time period 0.1 s to 0.5 s. Due to this disturbance, the simulation results of test system with and without CSC-STATCOM are shown in Figs. 12 to 17. Clearly,

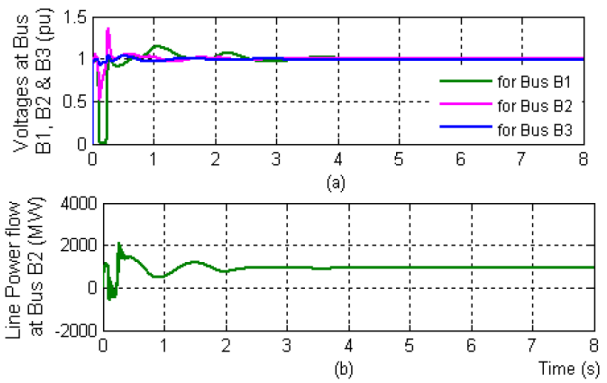

Fig. 8. Test-system response with CSC-STATCOM for a three phase fault (Case-I). (a) Positive sequence voltages at different buses B1, B2 & B3 (b) Power flow at bus B2

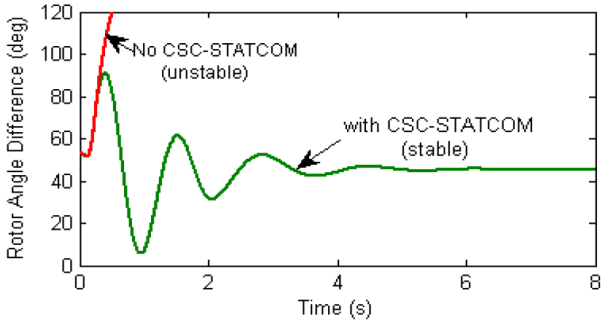

Fig. 9. Rotor angles difference of machines M1 & M2 for case-I

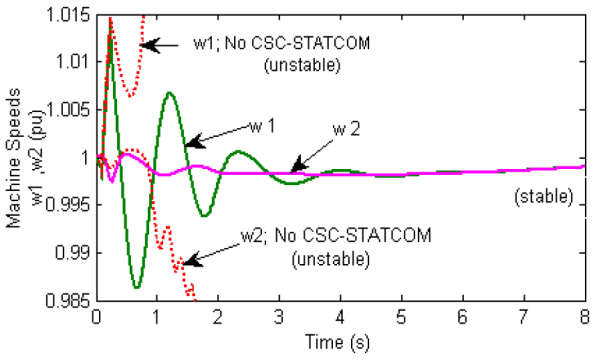

Fig. 10. Machine speeds w1 & w2 with CSC-STATCOM for case-I

the system becomes unstable in the absence of CSC-STATCOM due to this disturbance as in Figs. 12 & 15. But system with CSC-STATCOM is stable as observed in Figs. 14 to 17. Figure 17 also shows the amount of reactive power injected or absorbed by CSC-STATCOM

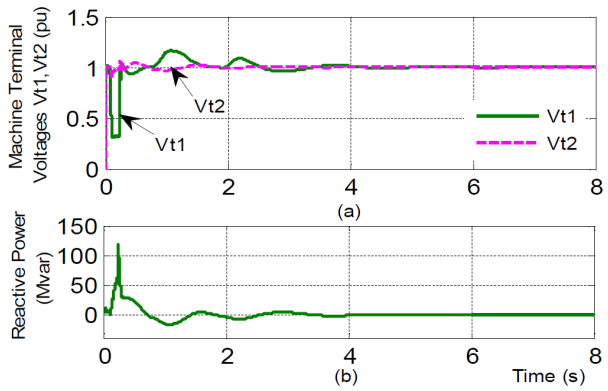

Fig. 11. For case-I (a) terminal voltages Vt1 & Vt2 of generators M1 & M2 with CSC-STATCOM respectively (b) reactive power inject (or absorb) by CSC-STATCOM

to the test system for maintaining the system stability. The CCT for the system with & without CSC-STATCOM are 585 ms & 442 ms respectively, which are provided in Table 1. Clearly, CCT for test system is better due to LQR based CSC-STATCOM. Hence the performance of CSC-STATCOM is satisfactory in this case also.

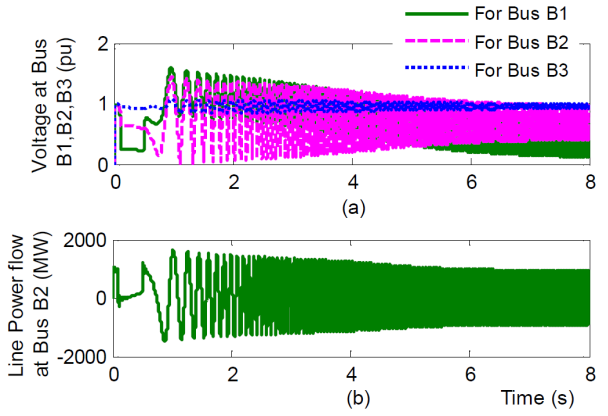

Fig. 12. The test system response without CSC-STATCOM for a heavy loading (Case-II). (a) Positive sequence voltages at different buses B1, B2 & B3. (b) Power flow at bus B2

4.4 Case III-A comparative study:

In order to demonstrate the robust performance of the proposed scheme for improving the transient stability of the system, outcomes from the proposed LQR based CSC-STATCOM are compared to that obtained from the other shunt FACTS devices such as SVC and VSC based STATCOM which have been reported in [24], [25]. It has been assumed that the test system is same for all shunt FACTS

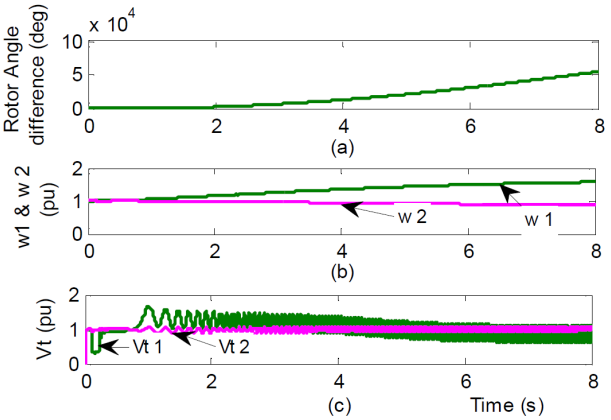

Fig. 13. System response without CSC-STATCOM for Case-II (a) Difference between Rotor angles of machines M1 & M2 (b) w1 & w2 speeds of machine M1 & M2 respectively (c)terminal voltages Vt1 & Vt2 of generators M1 & M2 respectively

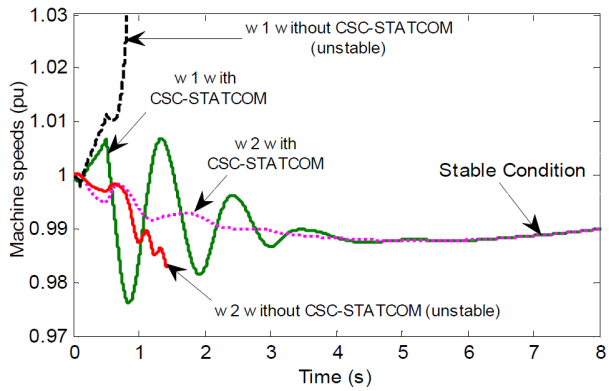

Fig. 14. Speeds w1 & w2 for machines M1 & M2 respectively for case-II

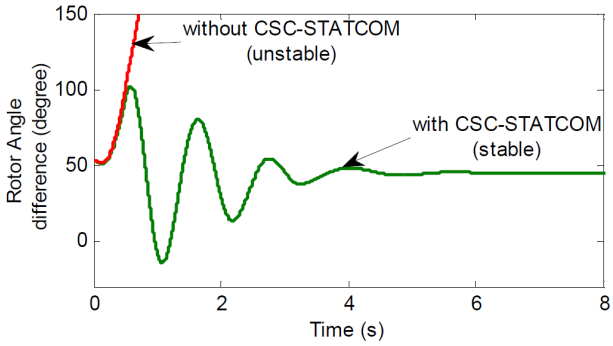

Fig. 15. Rotor angle difference of machines M1 & M2 for system with and without CSC-STATCOM in case-II

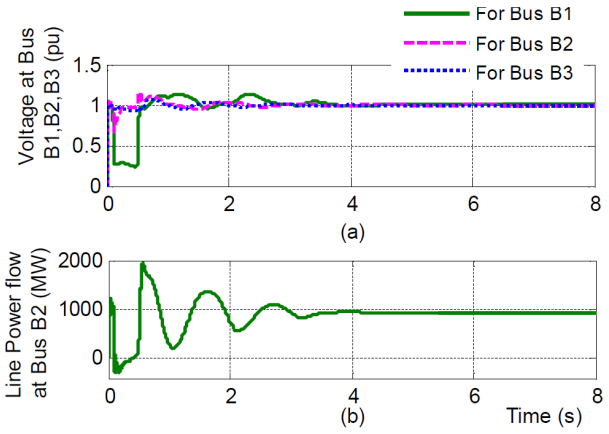

Fig. 16. The test system response with CSC-STATCOM for a heavy loading (Case-II). (a) Positive sequence voltages at different buses B1, B2 & B3. (b) Power flow at bus B2

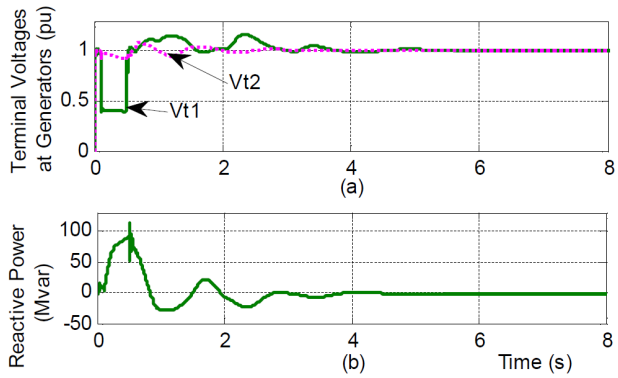

Fig. 17. For case-II (a) terminal voltages Vt1 & Vt2 of generators M1 & M2 with CSC-STATCOM respectively (b) reactive power inject (or absorb) by CSC-STATCOM

devices and all shunt FACTS devices have the same rating (200 Mvar). To check the impact of these shunt FACTS devices on the test system with three phase fault condition, simulation results with these shunt FACTS devices are compared in Fig. 18. The three phase fault duration is 0.1 s to 0.2 s. CCT for the system with different shunt FACTS devices are shown in Table-1. If three-phase fault duration is increased i.e. from 0.1 s to 0.24 s, then system with SVC becomes unstable. This is shown in Fig. 19. Waveforms show that CSC-STATCOM is more effective and robust than that of other shunt FACTS devices (SVC & VSC-STATCOM) in terms of oscillation damping, settling time, CCT and transient stability of the test-system in Figs. 18 & 19.

Table 1. CCT of disturbances for the test system stability with different shunt FACTS devices

S. No.	FACTS devices	Critical Clearing Time (CCT)
Case-I	Without CSC-STATCOM	100 ms – 222 ms
	With CSC-STATCOM	100 ms – 286 ms
Case-II	Without CSC-STATCOM	100 ms – 442 ms
	With CSC-STATCOM	100 ms – 585 ms
Case-III	With SVC	100 ms – 237 ms
	With VSC-STATCOM	100 ms – 240 ms
	With CSC-STATCOM	100 ms – 286 ms

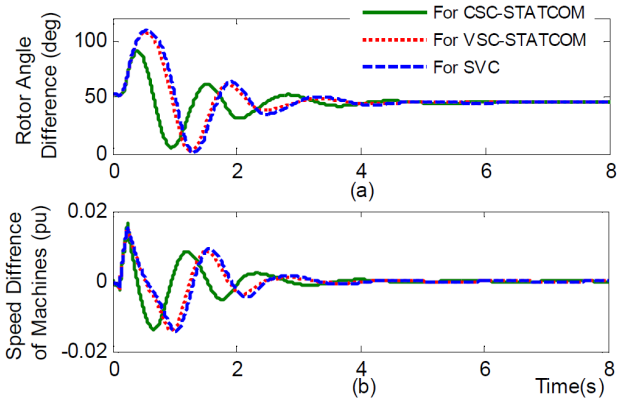

Fig. 18. System response with different shunt FACTS devices (CSC-STATCOM, VSC-STATCOM & SVC) for Case-III (a) Difference between Rotor angles of machines M1 & M2 (b) speed difference of machines M1 & M2

5 CONCLUSIONS

In this paper, a two cost function based LQR controller for the better input-output response of CSC-STATCOM is proposed in order to enhance the transient stability of the power system under various kinds of disturbances. The LQR based state feedback control technique is formulated and applied to the CSC-STATCOM. The dynamic modeling of CSC based STATCOM is presented. The LQR based CSC-STATCOM model is made independent of the operating point by applying the power balance equation. With the help of LQR based CSC-STATCOM, transient stability of a two-area two-machine power system is improved and CCT of disturbances are also increased. The proposed scheme is simulated and verified on MATLAB platform. This paper also compares the performance of CSC-

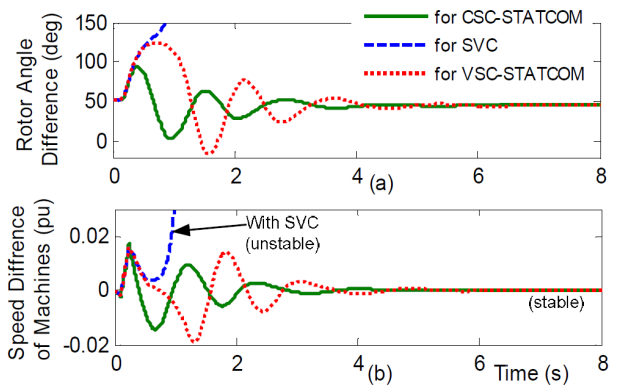

Fig. 19. System response with 3-phase fault for 0.1s to 0.24s in Case-III (a) Difference between Rotor angles of machines M1 & M2 (b) speed difference of machines M1 & M2

STATCOM with other shunt FACTS devices such as SVC & VSC-STATCOM in terms of oscillation damping, CCT and transient stability of two-area power system. It is observed that the CSC-STATCOM is more reliable and effective in comparison to these other FACTS devices. Hence, CSC based STATCOM can be regarded as an alternative FACTS device to that of other shunt FACTS devices i.e. SVC & VSC-STATCOM.

APPENDIX A

Parameters for various components used in the test system configuration of Fig. 5. (All parameters are in pu unless specified otherwise):

A.1 For generator of plant (P_1 & P_2):

$V_G = 13.8\,\text{kV}$; $R_s = 0.003$; $f = 50\,\text{Hz}$; $X_d = 1.305$; $X'_d = 0.296$; $X''_d = 0.252$; $X'_q = 0.50$; $X''_q = 0.243$; $T'_d = 1.01\,\text{s}$; $T''_d = 0.053\,\text{s}$; $H = 3.7\,\text{s}$. Where R_s is stator winding resistance of generators; V_G is generator voltage (L-L), f is frequency; X_d is synchronous reactance of generators; X'_d & X''_d are the transient and sub-transient reactance of generators in the direct-axis; X'_q & X''_q are the transient and sub-transient reactance of generators in the quadrature-axis; T'_d & T''_d are the transient and sub-transient open-circuit time constant; H the inertia constant of machine.

A.2 For Excitation System of machines (M1 & M2):

Regulator gain and time constant (Ka & Ta): 200, 0.001 s; Gain and time constant of exciter (Ke & Te): 1, 0 S; Damping filter gain and time constant (Kf & Tf): 0.001, 0.1 s; Upper and lower limit of the regulator output: 0, 7.

A.3 Parameters of shunt FACTS devices:

SVC:- System nominal voltage (L-L): $500\,\text{kV}$; f : $50\,\text{Hz}$; $K_p = 3$; $K_i = 500$; $V_{ref} = 1$.

VSC-STATCOM:- System nominal voltage (L-L): $500\,\text{kV}$; DC link nominal voltage: $40\,\text{kV}$; DC link capacitance: $0.0375\,\mu\text{F}$; f: $50\,\text{Hz}$; $K_p = 50$; $K_i = 1000$; $V_{ref} = 1$.

CSC-STATCOM:- System nominal voltage (L-L): $500\,\text{kV}$; $V_b = E_d$; $R_{dc} = 0.01\,\Omega$; $L_{dc} = 40\,\text{mH}$; $C_f = 400\,\mu\text{F}$; $R = 0.3\,\Omega$; $L = 2$ mH; $\omega = 314$; $V_{ref} = 1$.

REFERENCES

[1] Prabha Kundur, "*Power system stability and control*", McGraw-Hill, 1994.

[2] M. A. Abido, "Power system stability enhancement using FACTS controllers: a review," *The Arabian Journal for Science and Engineering*, Volume 34, Number-1B,pp. 153-172, April 2009.

[3] C.X. Dou, S.L. Guo, X.Z. Zhang, "Improvement of transient stability for power systems using wide-area measurement signals," *Electrical Engineering,* springer Publishing, vol. 91, pp. 133-143, 2009.

[4] X. D. Liu, Y. Li, Z. J. Liu, Z. G. Huang, Y. Q. Miao, Q. Jun, Q. Y. Jiang, and W. H. Chen, "A novel fast transient stability prediction method based on pmu," in *Power & Energy Society General Meeting*, pp. 1-5, 2009.

[5] R. J. Nelson, J. Bian, D. G. Ramey, T. A. Lemak, T. R. Rietman, and J. E. Hill, "Transient stability enhancement with FACTS controllers," in Proceedings of the 6th *International Conference on AC and DC Power Transmission*, pp. 269–274, May 1996.

[6] H. S. Hosseini, and A. Ajami, "Transient Stability Enhancement of AC Transmission System using STATCOM", *IEEE TENCON '02,* Vol. 3, pp.1809 - 1812, Oct. 2002.

[7] Y. L. Tan and Y. Wang,"A robust nonlinear excitation and SMES controller for transient stabilization", *International Journal of Electrical Power & Energy Systems,* vol. 26, no. 5, pp.325 -332 2004.

[8] M. H. Haque,"Improvement of first swing stability limit by utilizing full benefit of shunt facts devices", *IEEE Trans. Power Syst.*, vol. 19, no. 4, pp.1894 - 1902, 2004.

[9] N.C. Sahoo, B.K. Panigrahi, P.K. Dash and G. Panda, "Multivariable nonlinear control of STATCOM for

synchronous generator stabilization", *International Journal of Electrical Power & Energy Systems*, Volume 26, Issue 1, Pages 37–48, January 2004.

[10] H. Tsai, C. Chu and S. Lee, "Passivity-based Nonlinear STATCOM Controller Design for Improving Transient Stability of Power Systems", Proc. of *IEEE/PES Transmission and Distribution Conference & Exhibition*: Asia and Pacific Dalian, China, 2005.

[11] Arindam Chakraborty, Shravana K. Musunuri, Anurag K. Srivastava, and Anil K. Kondabathini, "Integrating STATCOM and Battery Energy Storage System for Power System Transient Stability: A Review and Application," *Advances in Power Electronics*, Hindawi Publishing, vol. 2012, Article ID 676010, 12 pages, 2012.

[12] Tan, Y.L, "Analysis of line compensation by shunt-connected FACTS controllers: a comparison between SVC and STATCOM," *IEEE Power Engineering Review*, vol. 19, no.8, pp. 57-58, 1999.

[13] B. Singh , R. Saha , A. Chandra and K. Al-Haddad, "Static synchronous compensators (STATCOM): A review", *IET Power Electron.,* vol. 2, no. 4, pp.297 -324, 2009.

[14] N. G. Hingorani and L. Gyugyi, *Understanding FACTS: Concepts and Technology of Flexible ac Transmission Systems*, IEEE Press, New York, 1999.

[15] B. Han and S. Moon, "Static synchronous compensator using thyristor PWM current source inverter", *IEEE Transactions Power Delivery,* vol. 15, pp.1285, 2000.

[16] Sandeep Gupta, R. K. Tripathi, "Voltage Stability Improvement in Power Systems using FACTS Controllers: State-of-the- Art Review", *IEEE International Conference on Power, Control and Embedded Systems* (ICPCES), pp.1-8, 2010.

[17] H.F. Bilgin, M. Ermis, "Current source converter based STATCOM: Operating principles, design and field performance," *Electric Power Systems Research*, Volume 81, Issue 2, Pages 478–487, February 2011.

[18] D. Shen and P. W. Lehn "Modeling, analysis, and control of a current source inverter-based STATCOM", *IEEE Transactions Power Delivery*, vol. 17, pp.248, 2002.

[19] M. Kazearni and Y. Ye "Comparative evaluation of three-phase PWM voltage- and current-source converter topologies in FACTS applications", *Proc. IEEE Power Eng. Soc. Summer Meeting*, vol. 1, pp.473, 2002.

[20] Y. Ye, M. Kazerani, Victor H. Quintana, "Current-Source Converter Based STATCOM: Modeling and Control", *IEEE Transactions on Power Delivery*, vol.20, no.2, April 2005.

[21] Y. Ni, L. Jiao, S. Chen and B. Zhang, "Application of a Nonlinear PID Controller on STATCOM with a Differential Tracker," *International Conference on Energy Management and Power Delivery*, EMPD-98, New York, USA, pp. 29-34, 1998.

[22] S. Gupta, R. K. Tripathi, "Two-Area Power System Stability Improvement using a Robust Controller based CSC-STATCOM", *Acta Polytechnica hungarica*, vol. 11/7, pp. 135-155, 2014.

[23] P. Rao , M. L. Crow and Z. P. Yang, "STATCOM control for power system voltage control applications", *IEEE Transactions Power Delivery*, vol. 15, no. 4, pp.1311 -1317, 2000.

[24] G. Sybille and P. Giroux, "Simulation of FACTS controllers using the MATLAB power system blockset and Hypersim real-time simulator", IEEE *Power Eng. Soc. Panel Session on Digital Simulations of FACTS and Custom Power Controllers*, Winter Meeting, p.p. 488-491, January 2002.

[25] Sidhartha Panda and Ramnarayan N. Patel,"Improving Power System Transient Stability with an Off–Centre Location of Shunt FACTS Devices," *Journal of Electrical Engineering*, vol. 57, No. 6, 365–368, 2006.

[26] C. Schauder and H. Mehta "Vector analysis and control of advanced static VAR compensators", *IEE Proceedings of Generation, Transmission and Distribution*, vol. 140, pp.299, 1993.

[27] Katsuhiko Ogata, "*Modern Control Engineering*", 5th Edition, Prentice Hall, 2010.

[28] B. T. Ooi , M. Kazerani , R. Marceau , Z. Wolanski , F. D. Galiana , D. McGillis and G. Joos "Midpoint sitting of facts devices in transmission lines", *IEEE Trans. Power Del.,* vol. 12, no. 4, pp.1717 - 1722, 1997.

Sandeep Gupta received the B.Tech. and M.E. degrees in Electrical Engineering in 2006 and 2009, respectively. Currently, he is an associate professor at Rajasthan Institute of Engineering & Technology Jaipur. He is also a research scholar at Motilal Nehru National Institute of Technology Allahabad-211004, India. His areas of interest in research are Application of artificial intelligence to power system control design, FACTS device, Power Electronics and stability of power system. He has been author and co-author of many papers published in journals and presented at the national and international conferences.

Ramesh Kumar Tripathi was born in Allahabad on August 01, 1969. He received the B.E. (Hons.) degree in electrical engineering from Regional Engineering College, Durgapur, University of Burdwan (W.B.), India, in 1989 and the M. Tech. Degree in microelectronics from Institute of Technology, Banaras Hindu University, Varanasi, India, in 1991. He received Ph.D. degree in power electronics from Indian Institute of Technology, Kanpur, India, in 2002. Currently he is Prof. & Head in the Department of Electrical Engineering, Motilal Nehru N.I.T. Allahabad, India. His research interests are Power Electronics, Reactive Power Control, Switch Mode Rectifiers, Power Quality, Active Power Filters and Virtual Instrumentation. He has been author and coauthor of many papers published in journals and presented at the national and international conferences.

AUTHORS' ADDRESSES

Sandeep Gupta
Department of Electrical Engineering,
Rajasthan Institute of Engineering & Technology
Jaipur - 303005, INDIA
Email: guptavilab@gmail.com

Prof. Ramesh K. Tripathi
Department of Electrical Engineering,
Motilal Nehru National Institute of Technology
Allahabad - 211004, INDIA
Email: rktripathi@mnnit.ac.in

Received: 2013-09-03
Accepted: 2014-02-15